Pergamon

Int. J. Mech. Sci. Vol. 39, No. 12, pp. 1315–1324, 1997

0020–7403/97 $17.00 + 0.00

PII: S0020–7403(97)00018–0

THE YIELD BEHAVIOUR OF METAL POWDERS

A. R. AKISANYA*, A. C. F. COCKS† and N. A. FLECK‡

* Engineering Department, Aberdeen University, King's College, Aberdeen AB24 3UE, U.K.,
† Engineering Department, Leicester University, University Road, Leicester LE1 7RH, U.K., and
‡ Engineering Department, Cambridge University, Trumpington Street, Cambridge CB2 1PZ, U.K.

(*Received* 24 *June* 1996; *and in revised form* 30 *October* 1996)

Abstract—Copper powders have been densified by cold hydrostatic compaction and by cold closed-die compaction. The stress versus strain relations were measured and the subsequent yield surfaces were probed. The shape of the yield surface is found to be sensitive to the type of compaction employed. Hydrostatic compaction results in a yield surface of approximately elliptical shape, while closed-die compaction produces a yield surface which is elongated along the loading direction with a vertex at the loading point. Existing theories of cold compaction are compared against the observed responses. © 1997 Elsevier Science Ltd.

Keywords: powder compaction, yield surfaces, triaxial tests.

1. INTRODUCTION

Powder metallurgy techniques have been employed in recent years to manufacture various complex shaped engineering components which are ordinarily difficult to cast or shape by other methods. Conventionally, two sequential processes are employed in the manufacture of a solid component. Firstly, loose powders are compacted in a suitably shaped die (closed-die compaction), or by using isostatic pressing, from an initial relative density D (=density of powder compact/full density of solid constituent) of 0.5–0.6 to a final relative density of 0.9–1. This process is referred to as cold or hot pressing depending upon whether the compaction occurs at room or elevated temperature, while the compacted powder is referred to as a "green compact". The green compact is then sintered; this involves heating the compact in a reducing atmosphere so that the particles bond together.

It is convenient to partition the densification process into two stages. At low relative densities, $D < 0.9$, densification is by the growth of localised necks between particles. This is termed "stage I" densification [1]. At higher relative densities, $D > 0.9$, the interconnected channels between the particles pinch-off leaving a network of isolated pores or voids within the body; the subsequent response is generally referred to as "stage II".

It is technologically important to have a good understanding of the constitutive law of an aggregate during state I compaction. The change in component dimension is much greater during stage I than in stage II compaction. Further, non-uniform stage I densification may result in the development of residual stresses and defects (for example, porosity variation and cracks), giving low green strength. These defects can cause premature failure during sintering of the green compact or during service of the component. In order to eliminate such defects constitutive laws are required for the compaction process. The present paper is concerned with the experimental determination of yield surface evolution for cold pressed powders in stage I ($D < 0.9$).

Various macroscopic constitutive models for powder compaction exist in the literature, see, for example, Refs [2–8]. Except for the work of Ashby and co-workers (for example, Ref. [1]) and Fleck [7, 8], which are based on the micro-mechanics of particle deformation, most of the other constitutive laws are quadratic functions of pressure and the von Mises effective stress. These empirical yield functions give elliptical yield surfaces in stress space, and are symmetric with respect to hydrostatic tension and compression. Moreover, the functions are isotropic in character, with the material response expressed in terms of a single-state variable, the relative density, D. Recent theoretical [8, 9] and experimental [10, 11] studies have shown that the yield behaviour of metal powder aggregates depends on both the relative density and the loading path.

The constitutive law proposed by Fleck [8] generates yield surfaces with features different from those of the earlier models (see, for example, Ref. [5]). Figure 1(a) shows Fleck's prediction of the

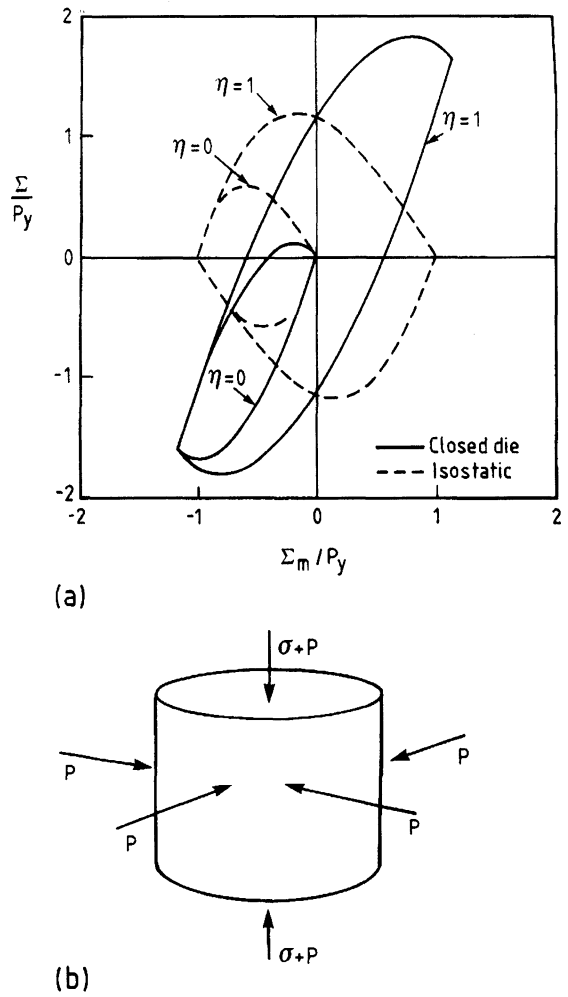

Fig. 1. (a) Effect of strain path on the evolution of yield surface at a relative density of $D = 0.8$. η is the ratio of the tensile cohesive strength to the compressive strength at the particle contact (from Ref. [8]). (b) A cylindrical powder compact subjected to an axisymmetric stress state.

yield surfaces for hydrostatic and closed-die compaction under axisymmetric loading, Fig. 1(b). In this figure $\Sigma_m = -(P + \sigma/3)$ is the mean stress and $\Sigma = -\sigma$ is proportional to the axial deviatoric component of stress. Both axes have been normalized by the macroscopic hydrostatic yield pressure P_y for cold isostatic compaction given by [6]

$$P_y \cong 3D^2 \frac{(D - D_0)}{(1 - D_0)} \sigma_y \tag{1}$$

where D_0 ($=0.64$) is the initial relative density for dense random packing, D is the relative density, and σ_y is the uniaxial yield strength for the solid composing the powder particles. The cohesion parameter η is the ratio of the tensile cohesive strength to the compressive strength at powder particle contacts. Thus, η is a measure of the level of particle cohesion: spherical shaped powders tend to be cohesionless (i.e. $\eta = 0$) while irregular shaped or sintered powders exhibit some level of cohesion and therefore have finite values of η. The shape of the yield surfaces shown in Fig. 1(a) are asymmetric with respect to hydrostatic tension and compression. Furthermore, the yield surfaces have sharp vertices at the initial loading points. For example, the yield surfaces for powder aggregates densified by hydrostatic compaction have vertices along the hydrostatic axis.

The successful industrial application of any constitutive model requires appropriate experimental validation of the model. Previous attempts to validate existing constitutive laws have been made either by compacting powders along a single proportional loading path or by measuring the yield

surface for sintered aggregates. For example, Kuhn and Downey [2] used uniaxial free compression tests for the calibration of their yield function, while Kim *et al.* [12] used combined torsion and compression test data on sintered specimens for calibrating their yield function. It has been shown by Brown and Weber [13] that the yield behaviour of compacted and then sintered powder is different from that of identical powder compacted without sintering; the uniaxial tensile yield stress is lower for compacted powder than for an identical powder which is compacted and then sintered. Furthermore, the use of isodensity curves as yield surfaces has been suggested [11, 14]. In general, isodensity curves do not coincide with yield surfaces because of the dependence of yield surfaces on the evolution of microstructure, such as pore shape [15, 16].

In this paper the yield surfaces of spherical copper powders are determined by probing the yield behaviour of a compacted powder specimen. A triaxial cell is used to compact circular cylindrical samples to a state of hydrostatic strain and to a state of uniaxial strain (as experienced in closed-die compaction). The triaxial cell is also used to determine the shape of the yield surface associated with a given compaction history. The experimental results are compared with existing constitutive laws, in particular, with the predictions of Fleck [8] shown in Fig. 1(a). We focus on the shape of the yield surface in the third quadrant, i.e. the case where both the mean stress and the axial deviatoric component of stress are compressive. The following section describes the experimental apparatus and procedures. We then present experimental yield data for the copper powder and discuss the practical implications of the experimental results.

2. EXPERIMENTAL METHODS

The material selected for this investigation is a gas atomized copper powder. The individual particles are spherical in shape and are of diameter in the range 50–65 μm see Fig. 2. Most of the particles have smaller particles attached to them. These smaller particles did not detach from the larger ones, even after prolonged agitation and vibration. Consequently, the loose packing relative density (D_0) of the powder particles is between 0.66 and 0.7. This is slightly greater than for random dense packing of $D_0 = 0.64$ since the smaller particles occupy some of the inter-particle pores.

A high-pressure triaxial system was used for the initial compaction and the subsequent probing of the yield surface. A sketch of the triaxial pressure cell is shown in Fig. 3. It consists of a pressure chamber and a piston rod for the application of axial force. Hydraulic fluid is used as the pressurising medium; the pressure cell has a maximum capacity of 100 MPa. In order to apply axial loading on the specimen, the triaxial cell was mounted in a screw-driven test machine with an axial load capacity of 100 kN.

A flexible rubber tube was filled with a measured mass of powder particles (roughly 0.020 kg), as shown in Fig. 3. Circular cylindrical specimens were used, of length 26 mm and diameter 12.5 mm.

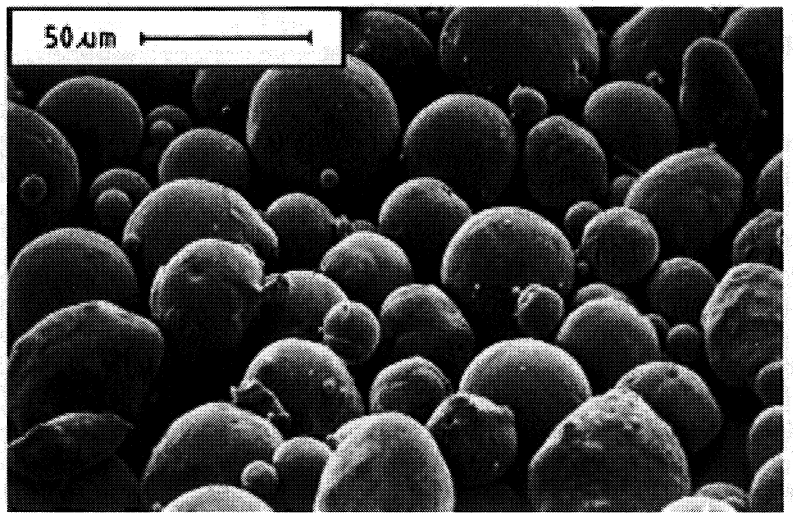

Fig. 2. Micrograph of the gas-atomised copper powder; the particles are relatively spherical in shape.

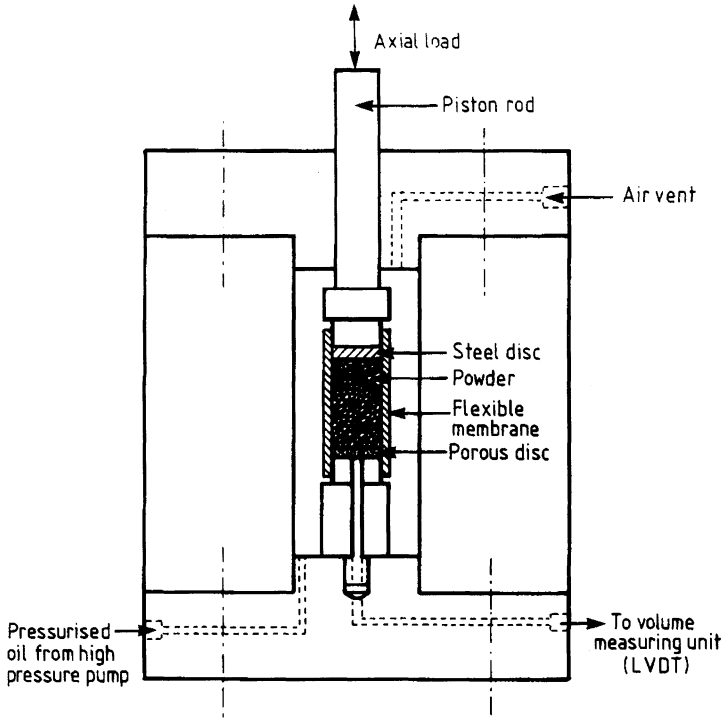

Fig. 3. A schematic of the triaxial pressure cell used for the probing of the yield surface.

A porous ceramic/metal disc was placed on the bottom face of the specimen and the powder was saturated with water for volume measurement; the water fills the inter-particle pores. A solid steel disc was placed on the top face of the specimen to prevent egress of water from the top face.

Axial loading was applied to the specimen via a piston rod, and the axial displacement was measured using a linear variable displacement transducer (LVDT) attached to the cell. Compaction of the specimen is accompanied by the forcing of water from the pores through the lower porous disc to an external column of water. The amount of displaced water resulting from the change in specimen volume was measured using a LVDT to determine the movement of a float placed on the top surface of the water column. This arrangement has a resolution of the order of 10^{-8} m^3, thus allowing the volumetric strain to be determined to within $\pm 0.3\%$. Recall that the pores are interconnected in stage I ($D < 0.9$) and they are isolated in stage II ($D > 0.9$). For values of relative density greater than 0.9, the isolated pores may contain some water resulting in the development of pore pressure with increasing densification. In this paper we focus on the behaviour of powder aggregates at low relative densities, i.e., $D < 0.9$. The triaxial cell test described above is similar to the conventional drained test method used in soil mechanics [17].

The axial force, axial displacement and the change in pore volume were recorded at set intervals of time using a computerised data logger. The relative density during compaction was calculated from the volume and mass of the specimen. For hydrostatic compaction, the confining pressure was incrementally increased and the corresponding change in volume of the specimen was recorded; no axial load was applied at this stage. Once the required density had been attained, the current yield surface was probed as follows. The hydrostatic pressure was decreased to a fixed value and the axial load was incremented until the onset of yielding of the specimen. A plot of axial load against axial displacement on an X–Y recorder was used to determine the onset of yielding. The change in relative density during the application of the axial load was minimal; the axial plastic strain during the probing operation was less than 0.01. The specimen was unloaded axially immediately after the onset of yielding. The pressure was then decreased and the probing process was repeated. The probing of the yield surface over a range of stress states was done on a single specimen at each relative density.

In the case of closed-die compaction, the inherent problem of die friction was avoided by simulating the state of strain in a closed die using the triaxial cell. Hydrostatic pressure and axial

load were applied alternately in small increments such that the accumulated volumetric strain and the axial strain were equal. This process was repeated until the required relative density was attained. In the present study the confining pressure was applied in increments of 5 MPa and the axial force was increased until the axial strain and the volumetric strain were equal.

The probing of the yield surface for closed-die compaction was carried out using two methods. The first method is similar to the one used for hydrostatic compaction, where the confining pressure was kept constant while the axial load was incremented until yielding occurred. In the second method, the axial load was set to an initial value and the corresponding crosshead displacement was kept constant while the fluid pressure was increased in small increments until yielding occurred. Thus, no additional axial strain was applied to the specimen while the confining pressure was incrementally increased. A plot of pressure increment against volumetric strain increment was used to determine the onset of yielding. Once the yield pressure has been determined, the pressure and the axial load were decreased and the process was repeated. As for hydrostatic compaction, we ensured that additional plastic deformation during probing was minimal, so there was only a negligible change in the relative density of the specimen. The determination of the onset of yield using both pressure and axial load increments provided us with more detailed information regarding the shape and evolution of the yield surface.

3. RESULTS

3.1. *Hydrostatic compaction*

Figure 4 shows the pressure P versus relative density D response during hydrostatic compaction for four specimens. The relative density increases with increasing hydrostatic pressure; the maximum relative density attained is $D = 0.895$ at a pressure of 100 MPa. Because of the morphology of the powder used in this study (see Fig. 2), the initial relative density $D_0 \approx 0.7$ is higher than the random close-packed value of $D_0 = 0.64$. The experimental results are compared with Ashby's [6] prediction [see Eqn (1)], assuming a uniaxial yield stress of $\sigma_y = 60$ MPa for pure copper powder [18] and an initial relative density of $D_0 = 0.7$. The predictions of the Ashby's model [6] compare favourably with the observed experimental pressure versus density response.

The probing of the yield surface for hydrostatic compaction was carried out by applying axial load at fixed values of confining pressure, as described in the previous section. Typical plots of axial stress versus axial strain are shown in Fig. 5 for the case of an initial hydrostatic compaction by a pressure of 100 MPa. The stress–strain relation at low values of confining pressure is initially non-linear up to a strain of about 0.2%, after which a linear relationship exists between the stress and strain until yielding occurs. The axial yield stress is determined using a 0.1% offset strain criterion from where the extrapolated linear segment of the stress–strain curve crosses the horizontal strain axis. We observed that all the specimens tested at zero confining pressure failed as soon as the axial load was applied. The axial stress at yield σ and the corresponding pressure P were used to calculate the mean

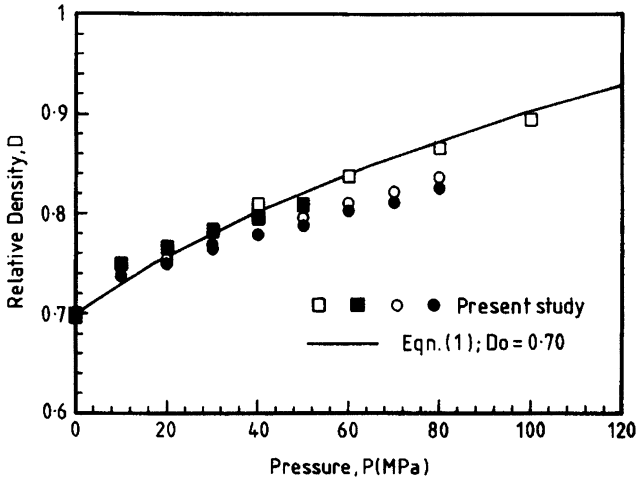

Fig. 4. Pressure–density response for the copper powder.

stress $\Sigma_m \equiv -(P + \sigma/3)$ and a scalar measure of the deviatoric stress $\Sigma \equiv -\sigma$ [see Fig. 1(b)]. A plot of the yield surfaces for three different values of relative density: $D = 0.81, 0.837$ and 0.895, is shown in Fig. 6, in $\Sigma_m - \Sigma$ space. All stresses are compressive, and thus, the experimental data are associated with the third quadrant of Fig. 1(a). The direction of the strain rate vector is indicated at the loading points for the powder compact with relative density $D = 0.837$. It is clear from the figure that plastic straining is normal to the yield surface. Note that the yield surfaces pass through the origin indicating that the cold compacted powder specimens cannot support any tensile hydrostatic stress.

The yield data are re-plotted in non-dimensional form in Fig. 7. Both axes have been normalized by the measured hydrostatic yield pressure P_y ($P_y = 60, 80$, and 100 MPa for $D = 0.81, 0.837$ and 0.895, respectively). Neglecting the slight scatter in the experimental data, the yield points for the three values of relative density collapse onto a single curve. We conclude that the yield surfaces are geometrically similar, and increase in size with increasing relative density.

The experimentally determined yield surfaces resemble the Cam-caly soil mechanics model developed by Schofield and Wroth [19], described by

$$\Phi(\Sigma_m, \Sigma) = \frac{\Sigma_m}{P_y}\left(\frac{\Sigma_m}{P_y} - 1\right) + \left(\frac{\Sigma}{MP_y}\right)^2 = 0 \tag{2}$$

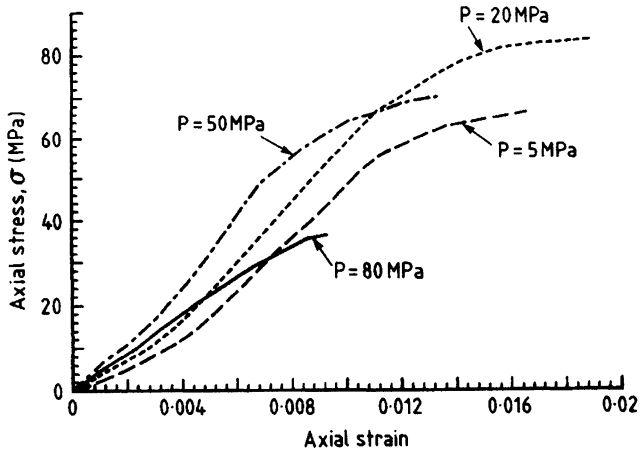

Fig. 5. Probing of the yield surface after hydrostatic compaction by a pressure of 100 MPa. The superposed axial stress σ is plotted against axial strain for fixed values of confining pressure P.

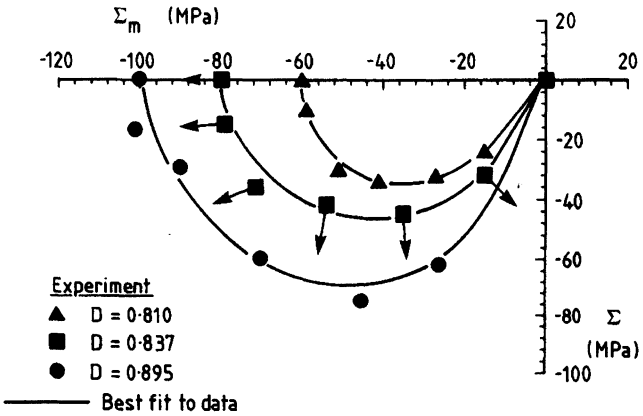

Fig. 6. Yield surfaces for an hydrostatic compact at various values of relative densities. The deviatoric stress $\Sigma \equiv -\sigma$ and the mean stress $\Sigma_m \equiv -(P + \sigma/3)$, where P is the fluid pressure and σ is the axial stress, at yield. The direction of the strain rate vector is indicated at the loading points for $D = 0.837$.

where P_y is the hydrostatic yield pressure [see Eqn (1)] and M is a constant controlling the shape of the surface. The Cam-clay type yield surface (using $M = 1.2$) is compared with the experimental results in Fig. 7: there is good agreement between the Cam-clay model and the experimental results.

For comparison purposes, we have also included in Fig. 7 predictions of the yield surface given by Fleck [8]. The experimental results are in good agreement with Fleck's prediction at low values of normalised mean pressure ($|\Sigma_m| \leqslant 0.5P_y$). However, at relatively larger values of mean pressure ($|\Sigma_m| > 0.5P_y$) the axial component of the deviatoric stress required to cause yielding is lower for Fleck's prediction than for the experimental results. Further, there is no observed vertex on the yield surface along the hydrostatic axis.

3.2. *Closed-die compaction*

The yield data for closed-die compaction are shown in Fig. 8. The experimental data were obtained from three different specimens. The data near to the deviatoric stress axis (curve A) are taken from a single specimen, and were obtained by incrementing the axial stress σ at a fixed value of confining pressure. The application of increasing hydrostatic pressure at a fixed crosshead displacement was used to obtain the data near to the hydrostatic axis (curve B), using two

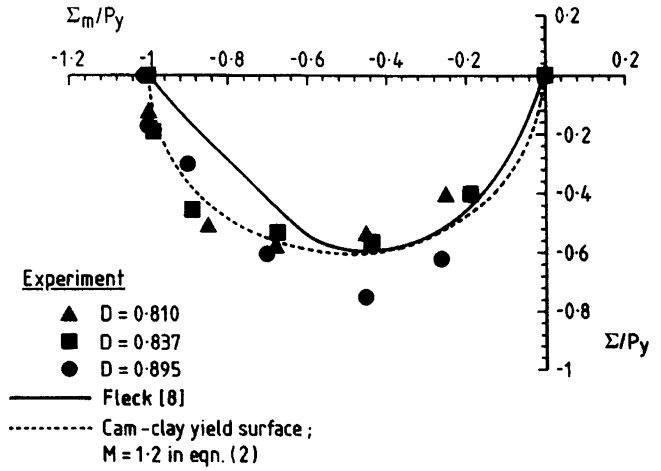

Fig. 7. Comparison of the experimental results for the yield surface with the predictions of Fleck [8] and Cam-clay type yield surface. P_y is the macroscopic yield pressure: $P_y = 60, 80$ and 100 MPa for $D = 0.810, 0.837$ and 0.895, respectively.

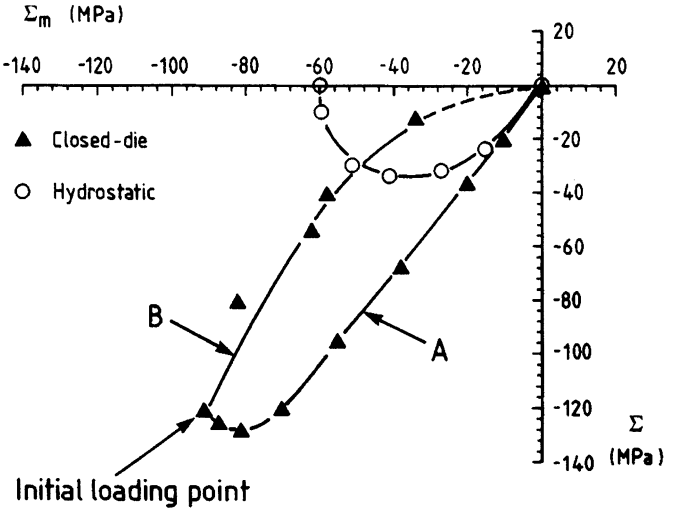

Fig. 8. Comparison between the yield surface for hydrostatic compaction and closed-die compaction at a relative density of $D \cong 0.81$. The solid lines are best fit to the experimental data.

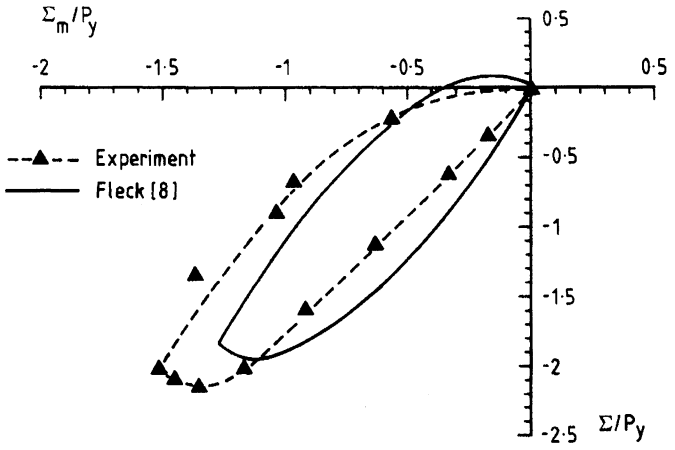

Fig. 9. Comparison of the Fleck [8] model of powder compaction with the experimentally determined yield surface after closed-die compaction. The stresses have been normalized by the hydrostatic stress P_y required to compact the aggregate isostatically to the same relative density $D = 0.82$.

specimens. For this method, a slight relaxation in the initial value of the axial stress was observed when the hydrostatic pressure was incrementally increased. Hence, the yield points were determined from the value of the hydrostatic pressure at yield and the corresponding value of the axial stress. The relative density is approximately 0.82 for all the three specimens, and there is good repeatability of the data.

For comparison purposes we have included in Fig. 8 the yield data for hydrostatic compaction at a relative density of $D = 0.81$. The deviatoric straining associated with closed-die compaction gives both larger particle contacts and a larger number of contacts along the axial direction than along other directions. This results in expansion of the yield surface in the direction of straining and a contraction in the transverse direction compared with the surfaces for hydrostatic compaction. As for hydrostatic compaction, the specimens failed at low values of confining pressure ($P < 5$ MPa) as soon as the axial stress σ was applied:

The yield data for closed-die compaction are re-plotted in Fig. 9, again using a non-dimensional scale; both the mean stress Σ_m and the deviatoric component of stress Σ have been normalized by the hydrostatic yield pressure P_y. We include Fleck's [8] prediction of the yield surface in Fig. 9, for a strain-hardening solid (of strain-hardening exponent $N = 0.3$). The experimental results give a slightly stronger response than the theoretical prediction. Unlike the yield surface for hydrostatic compaction, a vertex is observed at the initial loading point for closed-die compaction, in agreement with the prediction. It is not yet clear why a vertex is observed for closed-die compaction and not for hydrostatic compaction.

4. CONCLUDING DISCUSSION

We have obtained the yield surface of spherical copper powder initially densified by either hydrostatic compaction or closed-die compaction. The experimental results suggest that the yield surfaces for hydrostatic compaction are well represented by a Cam-clay-type yield model. The yield surface expands and maintains the same shape, with increasing values of relative density. However, the yield surface for closed-die compaction develops a vertex at the initial loading point, and it is elongated along the direction of straining. Thus, constitutive laws based on a single-state variable, for example, the relative density, are not adequate for describing the yield behaviour of powder aggregates.

The yield surfaces presented in this paper are applicable only to the two types of loading considered: hydrostatic compaction and closed-die compaction. In a general loading situation where the densifying material may experience a more complex stress state and histories, appropriate constitutive laws are needed to fully characterise the structure and the macroscopic response of the material. The constitutive law may depend on one or more state variables.

It is important to point out that Fleck's [8] analysis assumes isolated deformation at the particle contacts. The assumption of isolated deformation is only valid in the early stages of densification and interaction of the plastic zones with the free surface of the particle and with other deformation zones occurs as the material densifies further. The full effect of such interactions on the yield behaviour of spherical particles is still to be evaluated, but initial numerical studies on hexagonal arrays of cylinders [9, 16] and on the axisymmetric compaction of spherical particles [21] indicate that interaction of the plastic zones results in a net softening of the material response compared to the prediction of an isolated contact model.

In this paper the volumetric strain (and hence the relative density) was measured by saturating the powder specimens with water. For the uniformly spherical copper powder and the range of loading considered, there is little or no cohesion between the powder particles with or without the addition of water to the specimen. This is consistent with recent experimental results by Brown and Abou-Chedid [11] where unsaturated spherical powders are shown to have limited strength in uniaxial free compression. Cohesion between powder particles becomes important in irregularly shaped particles and in sintered powder components. The addition of water to the specimen may, however, influence the interparticle frictional sliding. Fleck [8] has shown that interparticle friction has negligible effect on the yield surface of powder aggregates. We therefore believe that the yield behaviour of the spherical copper powders saturated with water as examined in this paper is representative of that of 'dry' copper powders.

We have presented the yield data for only one quadrant (i.e. the third quadrant of Fig. 1). Experimental data for the second quadrant (compressive mean stress and tensile deviatoric stress) will provide information on the importance of the third invariant of stress. Yield data in the first and fourth quadrants where the hydrostatic stress is tensile can be obtained by using specimens which exhibit a significant among of cohesion between the particles, for example, by using a powder with irregular shaped particles.

Acknowledgements—This work was supported by a contract (N00014-91-J-4089) with the Advanced Research Projects Agency and the Office of Naval Research through a collaborative programme with the University of Virginia. Additional support was provided by N.I.S.T. ARA acknowledges the financial support of Aberdeen University Engineering Department. The authors wish to thank Dr John Cook of Schlumberger Research, Cambridge, for experimental assistance, and Dr Geoffrey Gretham of Manganese Bronze for supplying the powders.

REFERENCES

1. Helle, H. S., Easterling, K. E. and Ashby, M. F., Hot-isostatic pressing diagrams: new developments. *Acta Metallurgica*, 1985, **33**, 2163.
2. Kuhn, H. A. and Downey, C. L., Deformation characteristics and plasticity theory of sintered powder materials. *International Journal of Powder Metallurgy*, 1971, **7**, 15.
3. Green, R. J., A plasticity theory for porous solids. *International Journal of Mechanical Sciences*, 1972, **14**, 215.
4. Shima, S. and Oyane, M., Plasticity theory for porous metals. *International Journal of Mechanical Sciences*, 1976, **18**, 285.
5. Doraivelu, S. M., Gegel, G. L., Gunasekera, J. S., Malas, J. C. and Morgan, J. T., A new yield function for compressible P/M materials. *International Journal of Mechanical Sciences*, 1984, **26**, 527.
6. Ashby, M. F., *Background Reading: Hot isostatic Pressing and Sintering*. Internal Report, Cambridge University Engineering Department, Cambridge, 1990.
7. Fleck, N. A., Kuhn, L. T. and McMeeking, R. M., Yielding of metal powder bonded by isolated contacts. *Journal of Mechanics. Physics of Solids*, 1992, **40**, 1139.
8. Fleck, N. A., On the cold compaction of powders. *Journal of the Mechanics and Physics of Solids*, 1995, **43**, 1409.
9. Akisanya, A. R. and Cocks, A. C. F., Stage I compaction of cylindrical particles under nonhydrostatic loading. *Journal of Mechanics. Physics of Solids*, 1995, **43**, 605.
10. Watson, T. J. and Wert, J. A., On the development of constitutive relations for metallic powders. *Metallurgical Transactions A*, 1993, **24A**, 2071.
11. Brown, S. B. and Abou-Chedid, G., Yield behaviour of metal powder assemblages. *Journal of the Mechanics and Physics of Solids*, 1994, **42**, 383.
12. Kim, K. T., Suh, J. and Kwon, Y. S., Plastic yield of cold isostatically pressed and sintered porous iron under tension and torsion. *Powder Metallurgy*, 1990, **33**, 321.
13. Brown, S. B. and Weber, G. G. A., A constitutive model for the compaction of metal powders. *Modern Developments in Powder Metallurgy*, 1988, **18**, 465.
14. Gurson, A. L. and McCabe, T. J., Experimental determination of yield functions for compaction of blended metal powders. *Proceedings of the MPIF/APMI World Congress on Powder Metallurgy and Particulate Materials*, San Francisco, CA, 133, 1992.

15. Liu, Y. M., Wadley, H. N. G. and Duva, J. M., Densification of porous materials by power law creep. *Acta Metallurgica et Materialia*, 1994, **42**, 2247.
16. Akisanya, A. R., Cocks, A. C. F. and Fleck, N. A., Hydrostatic compaction of cylindrical particles. *Journal of the Mechanics and Physics of Solids*, 1994, **42**, 1067.
17. Bishop, A. W. and Henkel, D. J., *The Measurement of Soil Properties in the Triaxial Test*. Arnold, London, 1957.
18. Ashby, M. F. and Jones, D. R. H., *Engineering Materials I: An Introduction to their Properties and Applications*. Pergamon Press, Oxford, 1989.
19. Schofield, A. and Wroth, C. P., *Critical State Soil Mechanics*. McGraw-Hill, New York, 1968.
20. Gillion, J., Bouvard, D., Stutz, P., Grazzini, H., Levaillant, C., Baudin, P. and Cescutti, J. P., On the rheology of metal powder during cold compaction. In *Proceedings of the International Conference on Powders and Grains*, ed. Biarez and Gourves, Clemont-Ferrand, France, 433, 1989.
21. Ogbonna, N. and Fleck, N. A., Compaction of an array of spherical particles. *Acta Metallurgica et Materialia*, 1995, **43**, 603.